Deficiency of Clusterin Exacerbates High-Fat Diet-Induced Insulin Resistance in Male Mice

Min Jung Kwon,* Tae-jin Ju,* Jung-Yoon Heo, Yong-Woon Kim, Jong-Yeon Kim, Kyu-Chang Won, Jae-Ryong Kim, Young Kyung Bae, In-Sun Park, Bon-Hong Min, In-Kyu Lee, and So-Young Park

Departments of Physiology (M.J.K., T.-j.J., J.-Y.H., Y.-W.K., J.-Y.K., S.-Y.P.), Internal Medicine (K.-C.W.), Biochemistry and Molecular Biology (J.-R.K.), and Pathology (Y.K.B.) and Aging-Associated Vascular Disease Research Center (T.-j.J., J.-Y.H., J.-R.K., S.-Y.P.), College of Medicine, Yeungnam University, Daegu 705-703, South Korea; Department of Anatomy (I.-S.P.), College of Medicine, Inha University, Incheon 400-712, South Korea; Department of Pharmacology (B.-H.M.), College of Medicine, Korea University, Seoul 136-705, South Korea; and Department of Internal Medicine (I.-K.L.), School of Medicine, Kyungpook National University, Daegu 700-712, South Korea

The present study examined the role of clusterin in insulin resistance in high fat-fed wild-type and clusterin knockout (KO) mice. The plasma levels of glucose and C-peptide and islet size were increased in clusterin KO mice after an 8-week high-fat diet. In an ip glucose tolerance test, the area under the curve for glucose was not different, whereas the area under the curve for insulin was higher in clusterin KO mice. In a hyperinsulinemic-euglycemic clamp, the clamp insulin levels were higher in clusterin KO mice after the high-fat diet. After adjusting for the clamp insulin levels, the glucose infusion rate, suppression of hepatic glucose production, and glucose uptake were lower in clusterin KO mice in the high fat-fed group. The plasma levels of clusterin and clusterin mRNA levels in the skeletal muscle and liver were increased by the high-fat diet. The mRNA levels of the antioxidant enzymes were lower, and the mRNA levels of nicotinamide adenine dinucleotide phosphate oxidase (NOX) 1 and cytokines and protein carbonylation were higher in the skeletal muscle and liver in clusterin KO mice after the high-fat diet. Palmitate-induced gene expressions of NOX1 and cytokines were higher in the primary cultured hepatocytes of clusterin KO mice compared with the wild-type mice. Clusterin inhibited the gene expression and reactive oxygen species generation by palmitate in the hepatocytes and C2C12. AKT phosphorylation by insulin was reduced in the hepatocytes of clusterin KO mice. These results suggest that clusterin plays a protective role against high-fat diet-induced insulin resistance through the suppression of oxidative stress and inflammation. **(*Endocrinology* 155: 2089–2101, 2014)**

Clusterin is a disulfide-linked heterodimeric glycoprotein composed of α- and β-subunits that is constitutively expressed in almost all mammalian tissues (1). Although a single gene encodes clusterin, 3 mRNA isoforms are translated into a variety of proteins that can be grouped into secreted and nuclear clusterin according to their localization (2, 3). Clusterin forms a high-density lipoprotein (HDL) complex with apolipoprotein A-1 (ApoA1) and is also incorporated into the soluble terminal complement complex in the plasma (4).

Clusterin is known to be involved in physiological processes, such as complementary activity, lipid transporta-

ISSN Print 0013-7227 ISSN Online 1945-7170
Printed in U.S.A.

Received September 17, 2013. Accepted March 18, 2014.
First Published Online March 31, 2014

* M.J.K. and T.-j. J. contributed equally to this work.

Abbreviations: Ad-CLU, adenovirus expressing clusterin; Ad-GFP, adenovirus expressing GFP; ApoA1, apolipoprotein A-1; ApoB, apolipoprotein B; AUC, area under the curve; 2-[^{14}C]DG, 2-deoxy-D-[1-^{14}C]glucose; FBP, fructose-1,6-bisphosphatase; FBS, fetal bovine serum; GFP, green fluorescent protein; G6P, glucose-6-phosphatase; GPx1, glutathione peroxidase 1; HDL, high-density lipoprotein; HGP, hepatic glucose production; HOMA-IR, homeostasis model assessment of insulin resistance; iNOS, inducible nitric oxide synthase; IPGTT, ip glucose tolerance test; NOX1, nicotinamide adenine dinucleotide phosphate oxidase 1; qRT-PCR, quantitative real-time PCR; ROS, reactive oxygen species; SOD, superoxide dismutase; TBST, tris-buffered saline with Tween-20.

tion, sperm maturation, and apoptosis (5). Moreover, epidemiological studies reveal that clusterin is associated with inflammatory and metabolic diseases, including diabetes, atherosclerosis, and cancer (6–9). The serum clusterin levels are increased in type 2 diabetes patients and positively correlated with the blood glucose levels (6, 9), whereas the clusterin levels in HDL are lower in individuals with reduced insulin sensitivity and a higher body mass index (10). Furthermore, the clusterin single nucleotide polymorphism in Japanese diabetic patients is associated with the prevalence of type 2 diabetes (11). Although the physiological role of clusterin and previous epidemiological studies indicate the close relationship between clusterin and insulin resistance or diabetes, there is no direct evidence suggesting the involvement of clusterin in insulin sensitivity.

Therefore, in this study, we examined whether clusterin is involved in insulin resistance in high fat-fed wild-type and clusterin knockout mice using a hyperinsulinemic-euglycemic clamp study.

Materials and Methods

Animals

Eight-week-old male C57BL/6 wild-type and clusterin knockout mice were used in these experiments. To generate clusterin knockout mice with a C57BL/6 genetic background, clusterin-deficient mice originally generated using a Swiss black genetic background were backcrossed onto the C57BL/6 strain for at least 7 generations (12, 13). Mice were housed in a room with a 12-hour light, 12-hour dark cycle, with lights-on at 7 AM and light-off at 7 PM. The mice were fed on a standard chow diet or a high-fat diet for 8 weeks and given ad libitum access to water. The chow diet provided 64% energy as carbohydrate, 20% as protein, and 16% as fat (AIN-93G; Feedlab). The high-fat diet provided 20% energy as carbohydrate, 20% as protein, and 60% as fat (HFD 60% calories; Feedlab). The study was conducted in accordance with the guidelines for the care and use of laboratory animals provided by Yeungnam University, and all of the experimental protocols were approved by the Ethical Committee of Yeungnam University.

Intraperitoneal glucose tolerance test (IPGTT)

After an 8-week high-fat diet, the mice were fasted overnight, and blood samples were collected for basal glucose and insulin levels. Glucose (1.5 g/kg body weight) was injected ip, and blood samples for glucose were collected at 15, 30, 60, 90, and 120 minutes, whereas blood samples for insulin were collected at 15 and 60 minutes. Glucose was measured with OneTouch blood glucose meters (LifeScan Europe).

Homeostasis model assessment of insulin resistance (HOMA-IR)

HOMA-IR was calculated with fasting glucose and insulin concentrations, using the following formula: fasting blood glucose (mg/dL) × fasting insulin (μU/mL)/405.

Hyperinsulinemic-euglycemic clamp

A hyperinsulinemic-euglycemic clamp study was performed as previously described (14). Briefly, 4 days before the experiments, a catheter (silicone tubing; Helix Medical) was inserted into the right internal jugular vein of the mice to deliver solutions. After overnight fasting, a 2-hour hyperinsulinemic-euglycemic clamp was performed with a primed (900 pmol/kg body weight), and continuous infusion of human regular insulin (Novolin, Novo Nordisk) at a rate of 15 pmol/kg^{-1}·min^{-1}, and 20% glucose was infused to maintain glucose at constant concentrations. Blood samples were collected from the tail vessel, and the plasma glucose levels were measured using a Beckman Glucose Analyzer 2 (Beckman). The basal and insulin-stimulated rates of the whole-body glucose uptake were estimated with a continuous infusion of [3-^{3}H] glucose (PerkinElmer Life and Analytical Sciences) for 2 hours before the clamps (0.05 μCi/min) and throughout the clamps (0.1 μCi/min), respectively. To estimate insulin-stimulated glucose uptake in individual tissues, 2-deoxy-D-[1-^{14}C]glucose (2-[^{14}C]DG) (PerkinElmer Life and Analytical Sciences) was administered as a bolus (10 μCi) at 75 minutes after the start of the clamps. At the end of the clamps, the mice were anesthetized, and the tissue samples were dissected and stored at −80 °C. The epididymal fat pads were excised and weighed, and fat mass was expressed as percentage of total body weight. The whole-body glucose uptake rate was determined as the ratio of the [^{3}H] glucose infusion rate (disintegrations per minute [dpm/min]) to the specific activity of plasma glucose (dpm/μmol). Hepatic glucose production (HGP) during the clamps was determined by subtracting the glucose infusion rate from the whole-body glucose uptake rate. The glucose uptake rate in individual tissues was calculated from the plasma 2-[^{14}C]DG profile and the tissue 2-[^{14}C]DG 6-phosphate content using MLAB (Civilized Software).

Plasma biochemicals

Plasma levels of free fatty acids (Wako Diagnostics), triglycerides (Sigma-Aldrich), and cholesterols (Asan Pharmaceutical) were measured with enzymatic colorimetric method. Plasma levels of insulin (Millipore), C-peptide (Alpco), clusterin (Uscn Life Science, Inc), and ApoA1 (Uscn Life Science, Inc) were measured by an ELISA according to manufacturer's instructions.

Generation of recombinant adenovirus

Adenoviruses expressing clusterin (Ad-CLUs) were generated as previously described (15). Briefly, the cDNA encoding rat clusterin was inserted into the *Bgl*II/*Xho*I sites of the pAd-Track-CMV shuttle vector, and then the resultant shuttle vector was electroporated into BJ5138 cells containing the AdEasy adenoviral vector. The recombinant adenoviral plasmids were transfected and amplified in human embryonic kidney-293. The efficiency of adenoviral infection was assessed using a recombinant Ad-CLU fused to green fluorescent protein (GFP) (data not shown). Control adenoviruses (adenovirus expressing GFP [Ad-GFP]) were prepared by the same method.

Cell cultures

For the primary culture of mice hepatocytes, livers were perfused with Ca^{2+}-free Krebs-Ringer's HEPES buffer, followed by perfusion with Krebs-Ringer's HEPES buffer containing $CaCl_2$ and 0.3 mg/mL collagenase IV (Sigma-Aldrich). The isolated

hepatocytes were filtered through 100-μm nylon mesh, counted, and tested for viability using trypan blue exclusion. Cells were plated on 0.2% gelatin-coated dishes in DMEM (Gibco), supplemented with 10% fetal bovine serum (FBS), 10 mg/mL insulin, glutamin, and antibiotics. After attachment, the medium was replaced with fresh DMEM without insulin. C2C12 cells (American Type Culture Collection) were cultured in DMEM supplemented with 10% FBS and 1% penicillin/streptomycin (Sigma-Aldrich). For differentiation, cells grown to 70% confluence were switched to differentiation media (DMEM with 2% FBS) and then cultured for 6 days, during which time the medium was changed every 2 days.

Flow cytometry

The C2C12 cells were treated with 1 μg/mL recombinant mouse clusterin (R&D Systems) for 1 hour and then treated with 500μM palmitate for 6 hours. Reactive oxygen species (ROS) generation was determined using flow cytometry. The reagents were obtained from Becton Dickinson and used according to the manufacturer's instructions. Briefly, the cells were treated with 20μM 2′,7′-dichlorofluorescein diacetate (Sigma-Aldrich) for 20 minutes in the dark and washed twice with cold PBS. 2′,7′-dichlorofluorescein diacetate-V-fluorescein isothiocyanate-conjugated cells were detected with the FACScanto II (Becton Dickinson).

Staining

Pancreas were fixed in 10% neutral buffered formalin, embedded in paraffin block, sectioned into 4-μm-thick sections, and stained with hematoxylin and eosin. The digital images were captured using ProgRes C14 plus microscope camera (Jenoptik AG), and the largest diameters from each islet were measured to calculate the mean diameter (ProgRes Capture Pro V 2.8.8; Jenoptik AG). For immunohistochemical staining for insulin, 4-μm-thick tissue sections were mounted on poly-L-lysine-coated slides. Endogenous peroxidase activity was inactivated by incubation of the sections in 4% H_2O_2 for 5 minutes. After rinsing the sections in PBS, the tissue sections were then incubated with primary antibody (1:200, polyclonal; Abcam) for 60 minutes at room temperature, and then visualization of positive staining was achieved with use of a DAKO EnVision Plus-HRP labeled polymer detection kit (DAKO) according to the manufacturer's instructions.

Western blotting

The antibodies for the phosphorylated AKT at serine-473 and AKT were obtained from Cell Signaling Technology. The antibody for inducible nitric oxide synthase (iNOS) was from BD Biosciences, the antibody for IL-6 was from Abcam, and the antibody for glyceraldehyde 3-phosphate dehydrogenase was from Santa Cruz Biotechnology, Inc. Western blotting was performed as previously described (16). Briefly, the tissue samples were homogenized in lysis buffer, and protein concentrations were determined by a Bradford assay (Sigma-Aldrich). The proteins were separated by SDS-PAGE and transferred to a polyvinylidene fluoride membrane (Millipore). After blocking the membrane with Tris-buffered saline with Tween-20 (TBST) solution, the membrane was incubated with the primary antibodies overnight at 4°C. The membrane was washed in TBST, incubated with an antirabbit IgG secondary antibody (BD Biosciences) for 1 hour at room temperature. The bands were visualized with a chemiluminescent detection reagent (Millipore).

Protein carbonylation

Protein carbonylation was measured with an OxyBlot Protein Oxidation Detection kit (Millipore) as previously described (17). Briefly, the tissues were homogenized in lysis buffer (iNtRON Biotechnology) with 50mM dithiothreitol, and 10 μg of protein were incubated with 2,4-dinitrophenylhydrazine to form the 2,4-dinitrophenyl hydrazone derivatives. Protein was separated by SDS-PAGE and transferred to a polyvinylidene fluoride membrane. After blocking with TBST containing 1% BSA, the membrane was incubated with primary antibody, specific to the 2,4-dinitrophenyl moiety of the protein, and then incubated with goat antirabbit IgG coupled to horseradish peroxidase. Carbonylated protein was visualized using an enhanced chemiluminescence detection reagent (Millipore).

Quantitative real-time PCR (qRT-PCR)

A qRT-PCR was performed as previously described (16). Briefly, 25-mg tissue samples were homogenized in TRI reagent (Sigma-Aldrich), and RNA was reverse transcribed to cDNA using a reverse transcription kit (Applied Biosystems). qRT-PCR was performed using the Real-Time PCR 7500 System and Power SYBR Green PCR Master Mix (Applied Biosystems) according to the manufacturer's instructions. The expression levels of β-actin were used for sample normalization. Each reaction mixture was incubated at 95°C for 10 minutes followed by 45 cycles of 95°C for 15 seconds, 55°C for 20 seconds, and 72°C for 35 seconds. The primer sequences were: β-actin (121 bp: forward, 5′-TGGACAGTGAGGCAAGGATAG-3′; reverse, 5′-TACTGCCCTGGCT CCTAGCA-3′), iNOS (71 bp: forward, 5′-CTCCTGCCTCATGCCATT-3′; reverse, 5′-TGTTCC TCTATTTTTGCCTCTTTA-3′), TNF-α (71 bp: forward, 5′-CT ACTCCCAGGTTCTCTTCAA-3′; reverse, 5′-GCAGAGAG-GAGGTTGACTTTC), IL-1β (71 bp: forward, 5′-GCCCATCC TCTGTGA CTCA-3′; reverse, 5′-AGTGCAGCTGTCTAAT GGGA-3′), IL-6 (71 bp: forward, 5′-GTCGGAGGC TTAA TTACACATG-3′; reverse, 5′-TCAGAATTGCCATTGCACA-3′), superoxide dismutase (SOD) (71 bp: forward, 5′-CTGC TCTAATCAGGACCCATT-3′; reverse, 5′-GTGCTCCCACA CGTCAATC-3′), glutathione peroxidase 1 (GPx1) (71 bp: forward, 5′-GAAGTGCGAAGTGAATGGTG-3′; reverse, 5′-TGGGTGTTGGCAAGGC-3′), clusterin (71 bp: forward, 5′-GCATACCTGCATGAAGTTCTAT G-3′; reverse, 5′-GTA GAAGGGTGAGCTCTGGTTT-3′), and nicotinamide adenine dinucleotide phosphate oxidase (NOX) 1 (71 bp: forward, 5′-GGCTGCTGGACACCTATGT-3′; reverse, 5′-AGATCCA-GAGGTTTGGGTACA-3′), fructose-1,6-bisphosphatase (FBP) (71 bp: forward, 5′-AGCCTTCTGAGAAGGATGCTC-3′; reverse, 5′-GTCCA GCATGAAGCAGTTGAC-3′), glucose-6-phosphatase (G6P) (71 bp: forward, 5′-TGTCTAAC CG-GCTTCAGTTG-3′; reverse, 5′-TAATCGCCTTTAACT-GGCTACT-3′), ApoA1 (100 bp: forward, 5′-CAGCGGCA-GAGACTATGTGT-3′; reverse, 5′-AACGGTTGAACCCAGA GTGT-3′), and apolipoprotein B (ApoB) (100 bp: forward, 5′-CAGCCATGGGCAACTTTAC-3′; reverse, 5′-TGGGCAACGAT-ATCTGATTG-3′).

Tissue lipid and ApoA1 levels

The lipids in the liver and skeletal muscle were extracted by a modified version of the method of Folch et al (18). Tissues were homogenized with 0.01% butylethylhydroxylate containing chloroform:methanol 2:1 solution. The same amount of chloroform:methanol 2:1 solution was added, and the mixtures were agitated for 2 hours in an orbital shaker at room temperature. After adding distilled water, the tubes were centrifuged for 10 minutes at 3000 rpm. Chloroform layers were collected, and same amount of chloroform solution containing 1% Triton X-100 was added. After drying the sample, 100 μL of distilled water were added. The triglyceride levels (Sigma-Aldrich) were determined by enzymatic colorimetric methods (Sigma-Aldrich). The total cholesterol and HDL-cholesterol content was measured using total cholesterol kit and HDL-cholesterol kit (Asan Pharmaceutical). For tissue ApoA1 determination, liver was homogenized with a glass homogenized in PBS, and the homogenates were centrifuged at 5000 *g*. The supernate was used in the assay according to manufacturer's instructions (Uscn Life Science, Inc).

Statistics

The results are expressed as the mean ± SEM. The differences among the groups were analyzed with a one-way ANOVA followed by Tukey's post hoc test. The differences between the 2 groups were analyzed with Student's *t* test. $P < .05$ was considered significant.

Results

Body weight, fat mass, and plasma biochemicals

The body weight, fat mass, and plasma levels of glucose, insulin, and lipid were not different between the wild-type and clusterin knockout mice in the chow-fed group. An 8-week high-fat diet increased the body weight and fat mass in both the wild-type and clusterin knockout mice, and there was no difference between the 2 groups (Table 1). The plasma levels of glucose and insulin was also increased by the high-fat diet in both the wild- type and clusterin knockout mice, and the plasma glucose levels were significantly higher in the clusterin knockout mice compared with wild-type mice in high fat-fed group. The plasma levels of free fatty acids, triglycerides, and total cholesterol were increased by the high-fat diet in both the wild-type and clusterin knockout mice, and they were not different between the 2 groups. The plasma levels of HDL cholesterol were significantly reduced by the high-fat diet in both groups, and there was no difference between the 2 groups (Table 1). The plasma levels of clusterin were increased by the high-fat diet in the wild-type mice. The plasma levels of ApoA1 were increased in the clusterin knockout mice, and high-fat diet did not significantly affect the ApoA1 levels (Table 1).

IPGTT and HOMA-IR

The blood glucose and plasma insulin levels were not different between the 2 groups in the chow-fed mice after overnight fasting. The high-fat diet increased the blood glucose levels in the wild-type and clusterin knockout mice. The blood glucose levels of the clusterin knockout mice were significantly higher than those of the wild-type mice. The plasma insulin levels were also increased in both the wild-type and clusterin knockout mice after the high-fat diet, and the plasma insulin levels tended to be higher in the clusterin knockout mice than in the wild-type mice ($P < .07$). After an ip injection of 1.5 g/kg glucose, the blood glucose levels were higher at 15, 30, 60, 90, and 120 minutes in the mice with the high-fat diet, and there was no difference between the wild-type and clusterin knockout mice. The area under the curve (AUC) for glucose showed the same pattern of change after the high-fat diet (Figure 1, A and B). The plasma levels of insulin were increased at 15 and 60 minutes in the wild-type and clus-

Table 1. Body Weight, Fat Mass, and Plasma Levels of Glucose, Lipids, and Apolipoproteins in High Fat-Fed Wild-Type and Clusterin Knockout Mice

	Chow diet		High-fat diet	
	Wild-type	Clusterin KO	Wild-type	Clusterin KO
Body weight (g)	30 ± 0.8	29 ± 0.9	37 ± 0.8[a]	38 ± 0.8[a]
Fat mass (% BW)	3.2 ± 0.28	2.7 ± 0.28	5.0 ± 0.24[a]	5.3 ± 0.24[a]
Glucose (mM)	7.8 ± 0.56	8.9 ± 0.23	10.3 ± 0.58[a]	12.6 ± 0.59[ab]
Insulin (pM)	40 ± 5.1	51 ± 4.0	263 ± 33[a]	392 ± 55[a]
Free fatty acids (mEq/L)	0.7 ± 0.02	0.7 ± 0.03	0.9 ± 0.04[a]	0.9 ± 0.06[a]
Triglycerides (mM)	0.7 ± 0.01	0.7 ± 0.01	1.8 ± 0.08[a]	2.0 ± 0.06[a]
Total cholesterol (mM)	1.9 ± 0.05	2.0 ± 0.02	2.6 ± 0.17[a]	2.9 ± 0.12[a]
HDL cholesterol (mM)	1.4 ± 0.02	1.3 ± 0.02	1.0 ± 0.03[a]	0.9 ± 0.03[a]
Clusterin (μg/mL)	123 ± 3.7		140 ± 3.5[a]	
ApoA1 (mg/dL)	133 ± 11.2	165 ± 6.4[a]	152 ± 6.5	168 ± 8.1[a]

The results are expressed as mean ± SE. Experimental cases in each group are 8–10. BW, body weight; KO, knockout.

[a] $P < .05$ vs chow-fed wild-type.

[b] $P < .05$ vs high fat-fed wild-type mice.

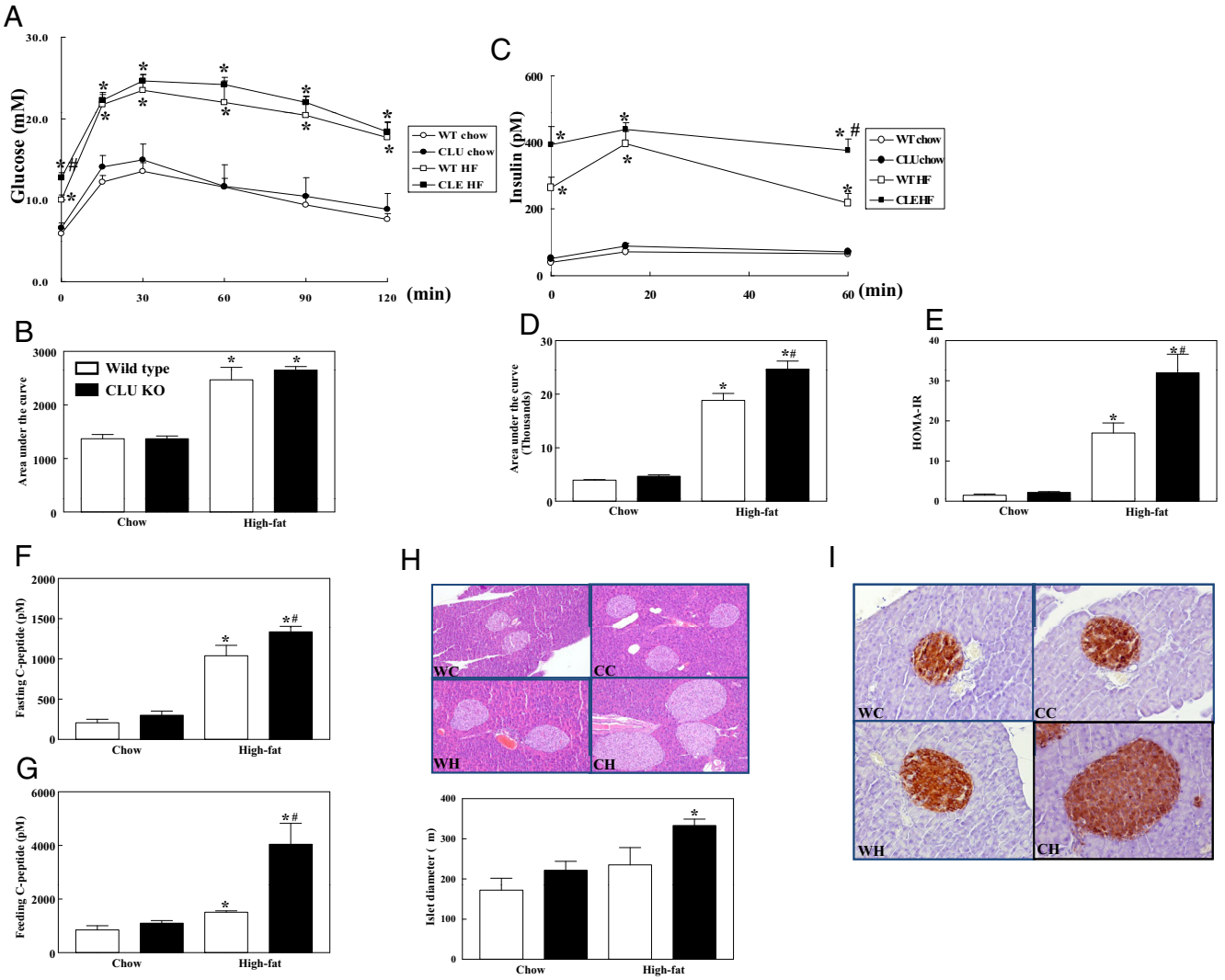

Figure 1. IPGTT and islet staining in the high fat-fed wild-type and clusterin knockout mice. After overnight fasting, the mice were injected with glucose (1.5 g/kg) ip, and the blood glucose (A) and insulin (C) were measured at the indicated time. The AUCs for glucose (B) and insulin (D) were calculated. HOMA-IR was calculated from glucose and insulin at 0 minutes (E). Plasma C-peptide levels after overnight fasting (F) and feeding (G). Pancreas was stained with hematoxylin-eosin, and the largest diameters from each islet were measured to calculate the mean diameter in the digital images (H). Immunohistochemical staining for insulin in pancreas (I). The results are expressed as the mean ± SE. Experimental cases in each group are 8–10. *, $P < .05$ vs chow-fed wild-type mice and #, $P < .05$ vs high fat-fed wild-type mice. WT, wild-type; CLU, clusterin; HF, high-fat; WC, wild-type chow; CC, clusterin knockout chow; WH, wild-type high-fat; CH, clusterin knockout high-fat; KO, knockout.

terin knockout mice after the high-fat diet, and the plasma levels of insulin in the clusterin knockout mice at 60 minutes were significantly higher than those of wild-type mice. The AUC for insulin was significantly higher in the clusterin knockout mice than in the wild-type mice (Figure 1, C and D). HOMA-IR was not different between the 2 groups in the chow-fed mice. The high-fat diet increased HOMA-IR in the wild-type mice and further increased HOMA-IR in the clusterin knockout mice (Figure 1E). The plasma levels of C-peptide after overnight fasting and feeding were not different between the wild-type and clusterin knockout mice in the chow-fed group. The high-fat diet increased the C-peptide levels in the wild-type and clusterin knockout mice, and the C-peptide levels were significantly higher in the clusterin knockout mice than those in the wild-type mice (Figure 1, F and G). The diameter of islets was significantly increased in the high fat-fed clusterin knockout mice compared with the chow-fed wild-type mice, and most of islet cells were positive for insulin (Figure 1, H and I).

Hyperinsulinemic-euglycemic clamp

The basal glucose uptake did not differ among the groups. The plasma insulin levels at basal state were higher in the high fat-fed mice, and there was no difference between the wild-type and clusterin knockout mice. During the hyperinsulinemic-euglycmic clamp, the plasma glucose levels were maintained at approximately 6mM in all groups, and the plasma

insulin levels were elevated to approximately 300pM in the chow diet group. The plasma insulin levels during the clamp were increased in the high fat-fed wild-type mice compared with those the chow-fed mice, and they were further increased in the high fat-fed clusterin knockout mice (Figure 2, A and B).

The glucose infusion rate to maintain euglycemia and whole-body glucose uptake were not different between the wild-type and clusterin knockout mice in the chow-fed group. The glucose infusion rate was reduced in both the wild-type and clusterin knockout mice after the high-fat diet, and there was no difference between the 2 groups (Figure 2C). The high-fat diet also reduced the insulin-stimulated whole-body glucose uptake in both the wild-type and clusterin knockout mice, and there was no difference between the 2 groups (Figure 2A). Because the clamp insulin levels were significantly higher in the clusterin knockout mice than in the wild-type mice after the high-fat diet, the glucose infusion rate and whole-body glucose uptake were adjusted for the clamp insulin levels. After the adjustment, the glucose infusion rate and whole-body glucose uptake were significantly reduced in the clusterin knockout mice compared with the wild-type mice in the high fat-fed group (Figure 2, D and E).

Glucose uptake in the skeletal muscle was not different between the 2 groups in the chow-fed mice. The high-fat diet reduced glucose uptake in both the wild-type and clusterin knockout mice, and there was no difference between the wild-type and clusterin knockout mice. After adjustment with the clamp insulin level, glucose uptake in the skeletal muscle was significantly lower in the clusterin knockout mice than in the wild-type mice in the high fat-fed group (Figure 3, A and B).

The suppression of HGP by insulin was not different between the 2 groups in the chow-fed mice. It was significantly reduced in both the wild-type and clusterin knockout mice after the high-fat diet, and there was no difference between the 2 groups. After adjustment with the clamp insulin levels, the suppression of HGP was significantly lower in the clusterin knockout mice compared with the wild-type mice in the high fat-fed group (Figure 3, C and D). The gene expression of G6P and FBP in the liver after hyperinsulinemic-euglycemic clamp was not different between the 2 groups in the chow-fed mice. The high-fat diet significantly increased the gene expression of these enzymes in the wild-type mice and further increased the gene expression of G6P ($P < .05$) and FBP ($P < .07$) in the clusterin knockout mice compared with the high fat-fed wild-type mice (Figure 3, E and F). The difference (Δ) in gene expression of G6P before and after insulin treatment was reduced in the wild-type mice after the high-fat diet, and it was further reduced in the high fat-fed clusterin knockout mice. The difference in gene expression of FBP was also reduced in the wild-type mice after the high-fat diet, and it tended to be further reduced in the high fat-fed clusterin knockout mice ($P < .07$ vs high fat-fed wild-type mice) (Figure 3, G and H).

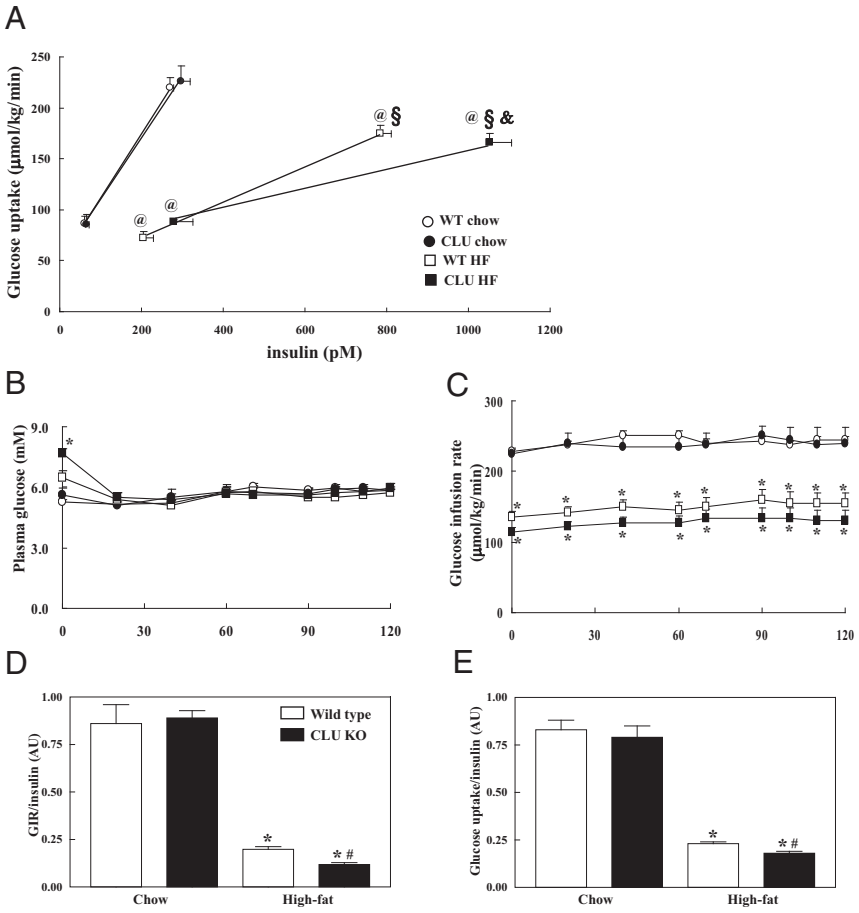

Figure 2. Hyperinsulinemic-euglycemic clamp study in the high fat-fed wild-type and clusterin knockout mice. Relation of the whole-body glucose uptake with the insulin levels at basal status and during the 2-hour clamp study (A). Plasma glucose levels during the clamp (B). Glucose infusion rate (GIR) during clamp (C). Adjusted GIR with clamp insulin (D). Adjusted whole-body glucose uptake with clamp insulin (E). The results are expressed as the mean ± SE. Experimental cases in each group are 8–10. *, $P < .05$ vs chow-fed wild-type mice and #, $P < .05$ vs high fat-fed wild-type mice; @, $P < .05$ vs corresponding chow-fed wild-type insulin; §, $P < .05$ vs chow-fed wild-type glucose uptake during clamp; &, $P < .05$ vs high fat-fed wild-type insulin during clamp. WT, wild-type; CLU, clusterin; HF, high-fat; KO, knockout.

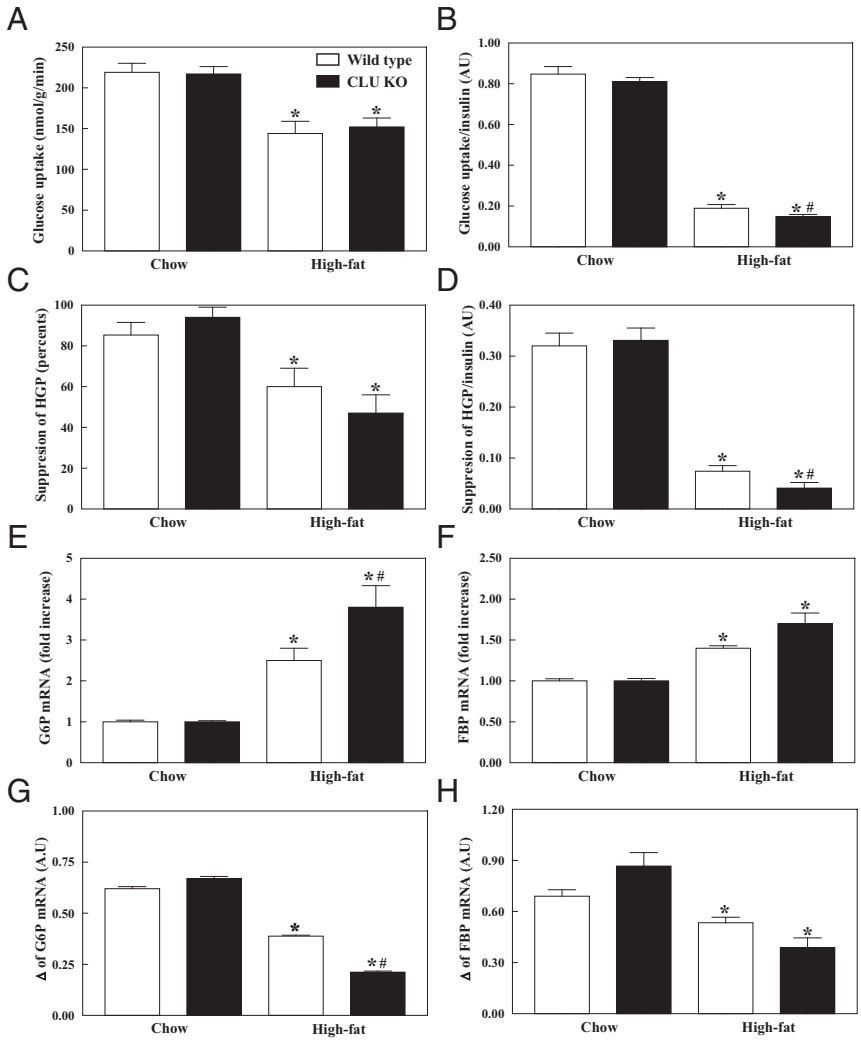

Figure 3. Glucose uptake in the skeletal muscle and suppression of HGP during the 2-hour hyperinsulinemic-euglycemic clamp in the high fat-fed wild-type and clusterin knockout mice. Glucose uptake in the skeletal muscle (A). Glucose uptake in the skeletal muscle was normalized with the clamp insulin levels (B). Suppression of HGP by insulin (C). Suppression of HGP was normalized with the clamp insulin levels (D). Gene expression of G6P (E) and FBP (F). The difference (Δ) in gene expression of G6P (G) and FBP (H) before and after insulin treatment. The difference of gene expression before and after insulin treatment was calculated by subtracting gene expression with insulin treatment from average value of gene expression without insulin treatment. The results are expressed as the mean ± SE. Experimental cases in each group are 8–10. *, $P < .05$ vs chow-fed wild-type mice and #, $P < .05$ vs high fat-fed wild-type mice. CLU, clusterin; KO, knockout.

Oxidative stress and inflammation in skeletal muscle

The gene expression of clusterin was increased in the skeletal muscle of the wild-type mice after the high-fat diet (Figure 4A). The gene expression of ApoA1 and ApoB was not different among the groups (Figure 4, B and C). The gene expression of NOX1 in the skeletal muscle was significantly increased in the clusterin knockout mice. The high-fat diet also increased the expression of NOX1 in the wild-type mice and further increased the gene expression in the clusterin knockout mice (Figure 4D). The gene expression of the antioxidant enzymes SOD and GPx1 was decreased in the wild-type mice after the high-fat diet, and it was further decreased in the clusterin knockout mice (Figure 4, E and F). Protein carbonylation in the skeletal muscle tended to be increased in the clusterin knockout mice ($P < .08$). The high-fat diet increased the protein carbonylation in the skeletal muscle of the wild-type mice and further increased the protein carbonylation in the clusterin knockout mice (Figure 4G). The gene expression of iNOS, IL-6, IL-1β, and TNF-α in the skeletal muscle was increased by the high-fat diet in the wild-type mice, and it was further increased in the clusterin knockout mice (Figure 4, H–K). The high-fat diet also increased the protein levels of iNOS and IL-6 in the wild-type mice and further increased the protein levels in the clusterin knockout mice (Figure 4, L and M).

Oxidative stress and inflammation in liver

The gene expression of clusterin in the liver was also increased by the high-fat diet in the wild-type mice (Figure 5A). The gene expression of ApoA1 was increased in the clusterin knockout mice, and high-fat diet had no significant effect on the ApoA1 mRNA levels. The ApoA1 protein levels showed the same pattern of change. The gene expression of ApoB was not affected by either high-fat diet or deficiency of clusterin (Figure 5, B–D). The gene expression of NOX1 was increased in the clusterin knockout mice compared with the wild-type mice in the chow-fed group. The high-fat diet increased NOX1 mRNA levels in the wild-type mice and further increased the gene expression in the clusterin knockout mice (Figure 5E). The gene expression of SOD and GPx1 was decreased in both the wild-type and clusterin knockout mice by the high-fat diet, and it was significantly lower in the clusterin knockout mice than in the wild-type mice (Figure 5, F and G). The high-fat diet increased protein carbonylation in the liver of the wild-type mice and further increased the protein carbonylation in the clusterin knock-

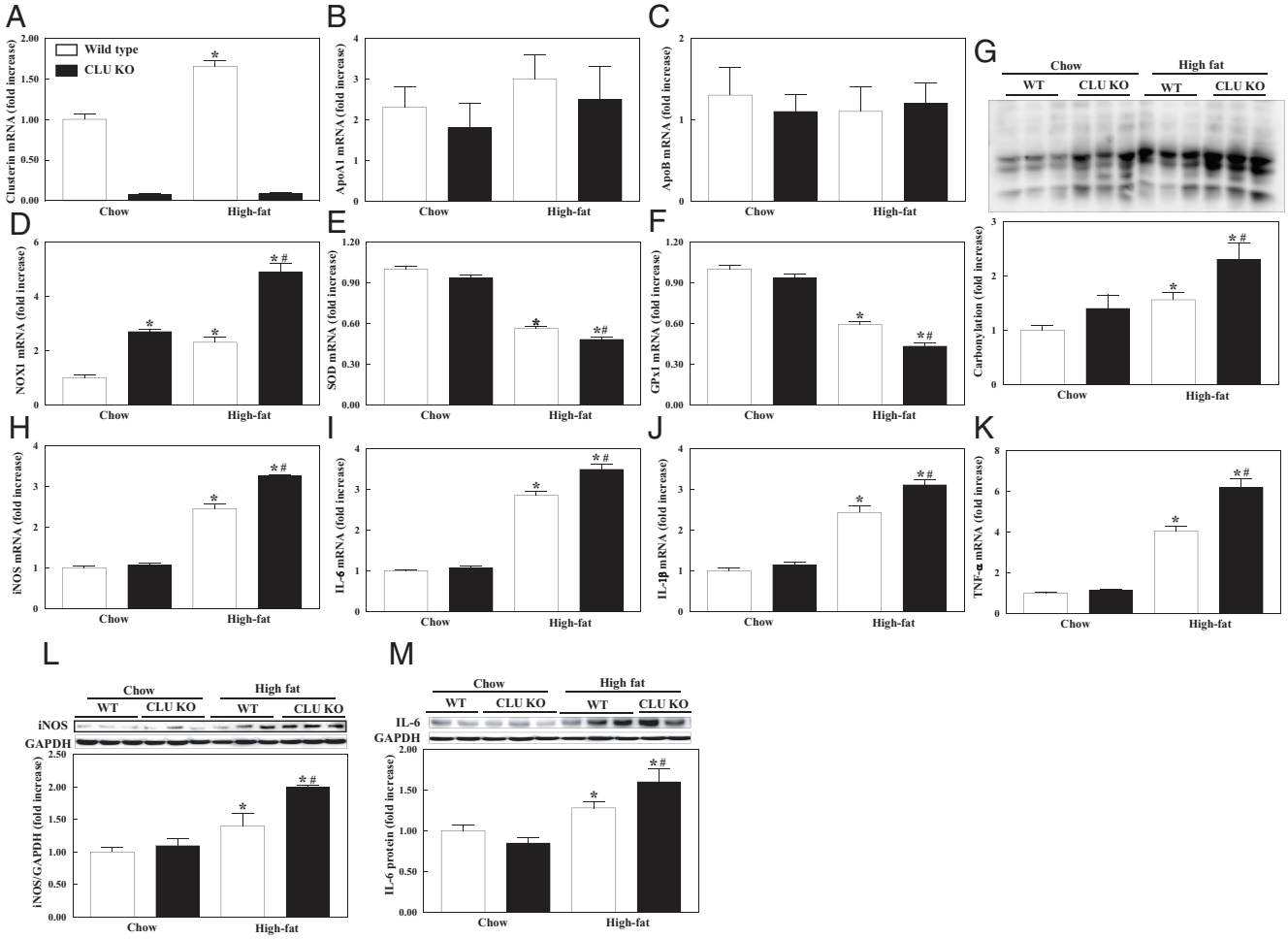

Figure 4. Expression of clusterin, apolipoprotein, prooxidant, antioxidant, and inflammatory cytokines in the skeletal muscle of the high fat-fed wild-type and clusterin knockout mice. Gene expression of clusterin (A), ApoA1 (B), ApoB (C), NOX1 (D), SOD (E), and GPx1 (F). Protein carbonylation (G). Gene expression of iNOS (H), IL-6 (I), IL-1β (J), and TNF-α (K). The protein levels of iNOS (L) and IL-6 (M). The results are expressed as the mean ± SE. Experimental cases in each group are 8–10. *, $P < .05$ vs chow-fed wild-type mice and #, $P < .05$ vs high fat-fed wild-type mice. WT, wild-type; CLU, clusterin; KO, knockout; GAPDH, glyceraldehyde 3-phosphate dehydrogenase.

out mice (Figure 5H). The gene expression and protein levels of iNOS were increased in both the wild-type and clusterin knockout mice by the high-fat diet, and they were significantly higher in the clusterin knockout mice than those in the wild-type mice. The gene expression and protein levels of IL-6 showed the same pattern of change with iNOS. The protein levels of IL-6 tended to be increased in the clusterin knockout mice compared with the wild-type mice after the high-fat diet ($P < .07$) (Figure 5, I–L).

Tissue lipid levels

Triglyceride, total cholesterol, and HDL-cholesterol levels in the skeletal muscle were not different between the 2 groups in the chow-fed mice. The high-fat diet increased the triglyceride and total cholesterol levels and decreased the HDL-cholesterol levels in the skeletal muscle both in the wild-type and clusterin knockout mice, and there was no difference between the 2 groups (Figure 6, A–C). Lipid levels in the liver showed a similar pattern of changes after the high-fat diet, and there was no difference between the 2 groups (Figure 6, D–F).

Oxidative stress, inflammation, and AKT phosphorylation in cells

Treatment of the hepatocytes with 500μM palmitate for 10 hours increased the mRNA levels of iNOS, IL-6, IL-1β, and TNF-α by 2-, 4-, 7-, and 1.7-fold, respectively, in the wild-type mice, whereas palmitate increased the gene expression of iNOS, IL-6, IL-1β, and TNF-α by 3-, 9-, 14-, and 3.3-fold, respectively, in the hepatocytes of clusterin knockout mice (Figure 7, A–D). Treatment of the hepatocytes from the wild-type mice with palmitate increased the gene expression of NOX1, iNOS, and IL-6, and clusterin overexpression using adenovirus (Ad-CLU) reduced the palmitate-induced gene expression (Figure 7, E–G). Treatment of the C2C12 myotubes with palmitate increased the gene expression of NOX1, iNOS, and IL-6, and clusterin treatment reduced the palmitate-induced

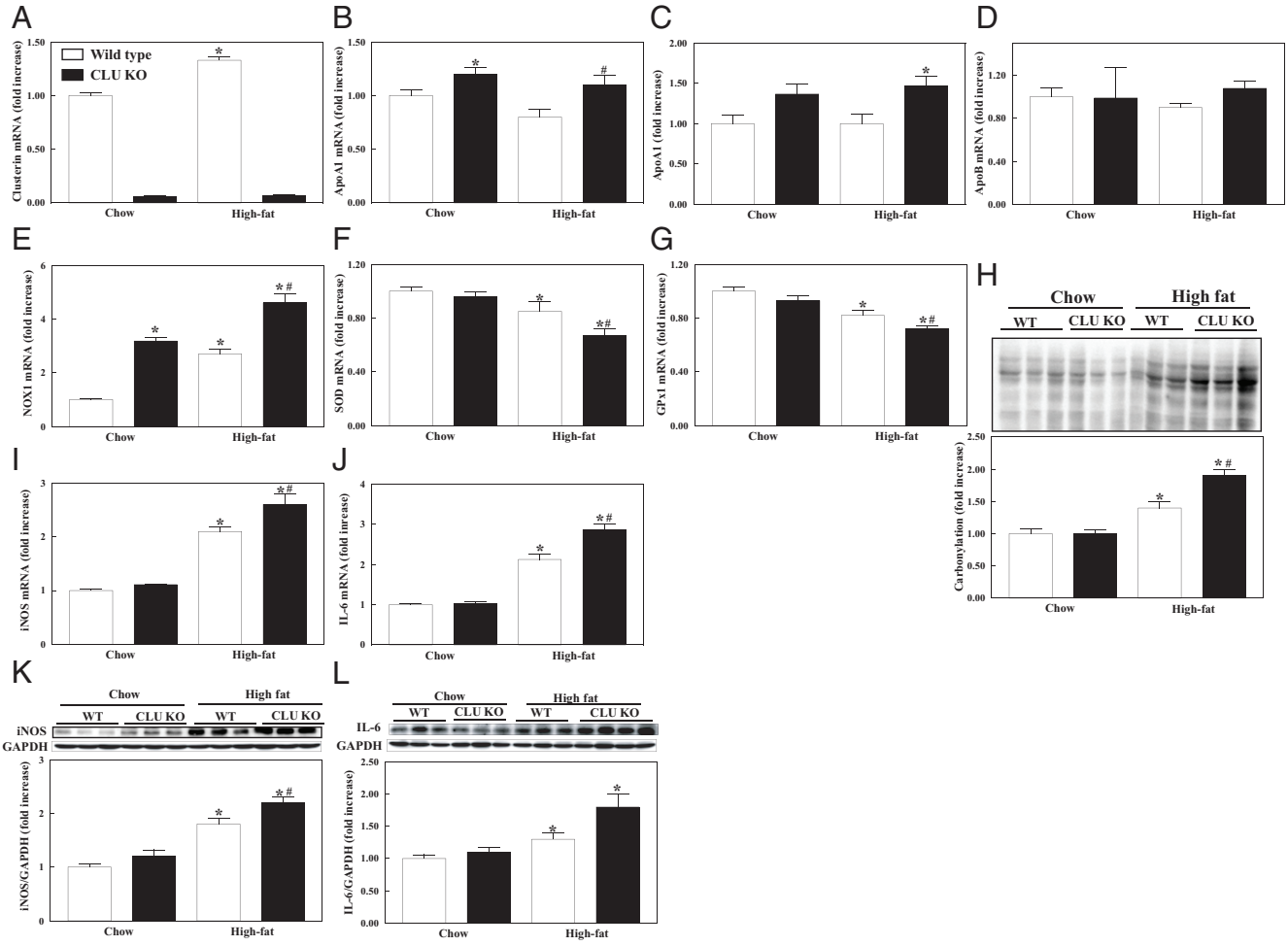

Figure 5. Expression of clusterin, apolipoprotein, prooxidant, antioxidant, and inflammatory cytokines in the liver of the high fat-fed wild-type and clusterin knockout mice. Gene expression of clusterin (A) and ApoA1 (B). ApoA1 protein levels (C). Gene expression of ApoB (D), NOX1 (E), SOD (F), and GPx1 (G). Protein carbonylation (H). Gene expression of iNOS (I) and IL-6 (J). Protein levels of iNOS (K) and IL-6 (L). The results are expressed as the mean ± SE. Experimental cases in each group are 8–10. *, $P < .05$ vs chow-fed wild-type mice and #, $P < .05$ vs high fat-fed wild-type mice. WT, wild-type; CLU, clusterin; KO, knockout; GAPDH, glyceraldehyde 3-phosphate dehydrogenase.

gene expression (Figure 7, H–J). Treatment of cells with 500μM palmitate for 6 hours increased ROS levels, and pretreatment of cells with 1 μg/mL clusterin reduced the palmitate-induced ROS generation in C2C12 (Figure 7K). Insulin-stimulated AKT phosphorylation at serine-473 was reduced in the hepatocytes of clusterin knockout mice, which was also observed in cells treated with palmitate (Figure 7L).

Discussion

The present study demonstrates that the high-fat diet induces insulin resistance and enhances clusterin expression, which is accompanied by increased oxidative stress and inflammation. A deficiency of clusterin exacerbates high-fat diet-induced insulin resistance and worsens oxidative stress and inflammation in mice. Clusterin treatment inhibits palmitate-induced ROS production and cytokine expression in cells, and insulin-stimulated AKT phosphorylation is reduced in clusterin-deficient cells. These results suggest that clusterin may have a protective role against high-fat diet-induced insulin resistance. Furthermore, they also indicate an association between clusterin and oxidative stress and inflammation after consumption of a high-fat diet.

Clusterin expression is increased in a variety of cells under stress conditions, including oxidative stress and inflammation. The gene expression of clusterin is increased by hydrogen peroxide in human fibroblasts (19), pancreatic acinar AR4–2J cells (20), and human epidermoid cancer cells (21). Lipopolysaccharides and inflammatory cytokines, such as TNF-α and IL-1, increase the hepatic mRNA levels and serum levels of clusterin in Syrian hamsters (22). Because obesity, induced by a high-fat diet, causes oxidative stress and inflammation (23, 24), it was assumed that a high-fat diet would increase clusterin ex-

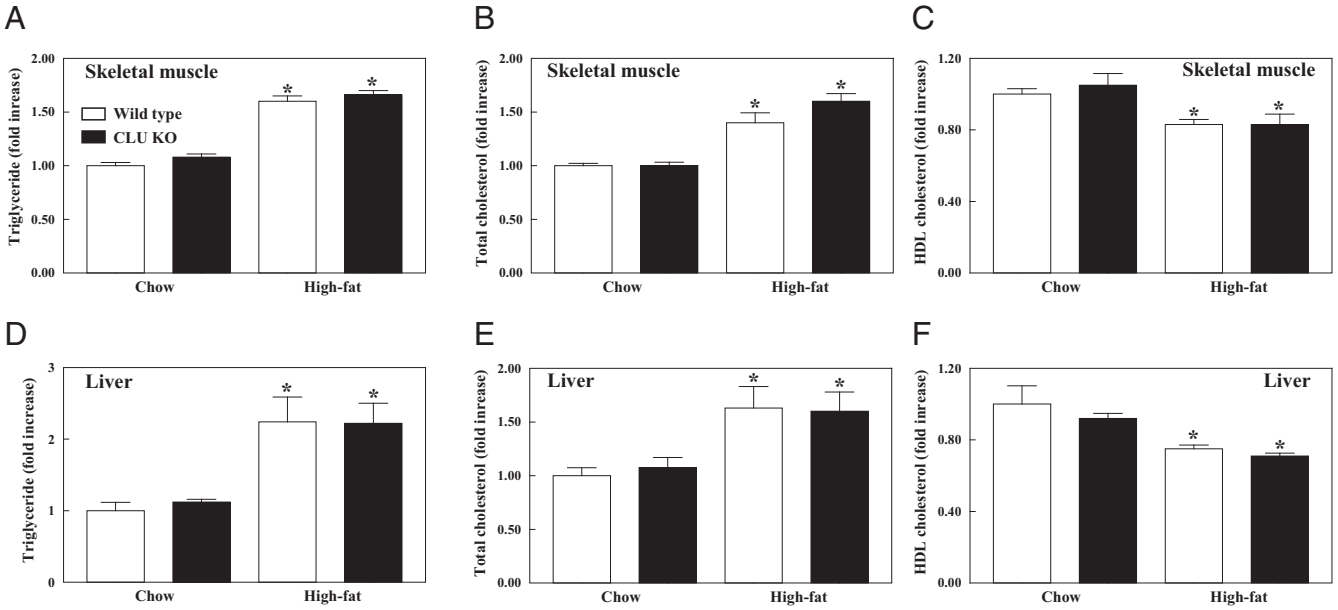

Figure 6. Lipid levels in the skeletal muscle and liver of the high fat-fed wild-type and clusterin knockout mice. Triglyceride (A), total cholesterol (B), and HDL cholesterol (C) in the skeletal muscle. Triglyceride (D), total cholesterol (E), and HDL cholesterol (F) in the liver. The results are expressed as the mean ± SE. Experimental cases in each group are 8–10. *, $P < .05$ vs chow-fed wild-type mice and #, $P < .05$ vs high fat-fed wild-type mice. CLU, clusterin; KO, knockout.

pression. As we expected, chronic high-fat feeding enhanced clusterin expression in the plasma and tissues, which was accompanied with increased oxidative stress and inflammation. Previously, clusterin is increased in the aortic lesions of the high fat-fed mice (25), and renal clusterin expression is higher in obese Zucker rats compared with age-matched lean strain (26). Weight loss by gastric bypass surgery reduces the plasma level of clusterin and the gene expression of clusterin in mononuclear cells in type 2 diabetes patients, which is accompanied by reduced proinflammatory mediators (27, 28).

Although increased levels of clusterin under oxidative stress may augment or retard the tissue damage, or may simply be a stress marker for oxidative stress, a line of evidence suggests the protective effects of clusterin on oxidative stress and inflammation. The overexpression of clusterin shows enhanced viability and less apoptosis in pancreatic acinar AR4–2J cells treated with hydrogen peroxide, whereas down-regulation of endogenous clusterin expression displays reduced viability and increased apoptosis (29). Increased clusterin expression suppresses the oxidative stress induced by other oxidants, such as UV and ethanol, and rescues the cells from apoptosis (21, 30, 31). Consistent with these previous results, clusterin suppressed the palmitate-induced ROS production and cytokine expression in the hepatocyte and C2C12 myotubes in the present study. Furthermore, the gene expression of clusterin is increased after pancreatitis induction in rats (20), and the clusterin knockout mice develop more severe pancreatitis (29). We also presently showed that a deficiency of clusterin presently exacerbated high-fat diet-induced oxidative stress and inflammation in mice. The antioxidant effect of clusterin is supported by thiol-reducing equivalents but not by acorbate in vitro, suggesting that clusterin inhibits ROS generation via its cysterin sulfhydryl groups (32). We also presently found that the ApoA1 levels were increased in the clusterin knockout mice. It seems that the increased ApoA1 expression is the compensatory response to a deficiency of clusterin, because ApoA1 is known to interact with clusterin and has antioxidant and antiinflammatory effects (33, 34),

Oxidative stress and inflammation induce insulin resistance via activation of c-Jun N-terminal kinase, which suppresses insulin-stimulated intracellular signaling pathways, including AKT phosphorylation (35, 36). The modulation of antioxidant enzymes improves or aggravates insulin resistance by the high-fat diet via affecting the oxidative stress. Increased oxidative stress with deletion of antioxidant enzymes, such as methionine sulfoxide A, aggravates high-fat diet-induced insulin resistance (37). The overexpression of SOD2 ameliorates high-fat diet-induced insulin resistance in rat skeletal muscle (23). Therefore, we suggest that a deficiency of clusterin results in increased oxidative stress and inflammation, which leads to aggravated insulin resistance in high fat-fed mice. In line with this suggestion, clusterin knockout mice demonstrated increased fasting glucose levels, HOMA-IR, and AUC of insulin during IPGTT. Moreover, the reduced activation of AKT by insulin in the hepatocytes of clusterin

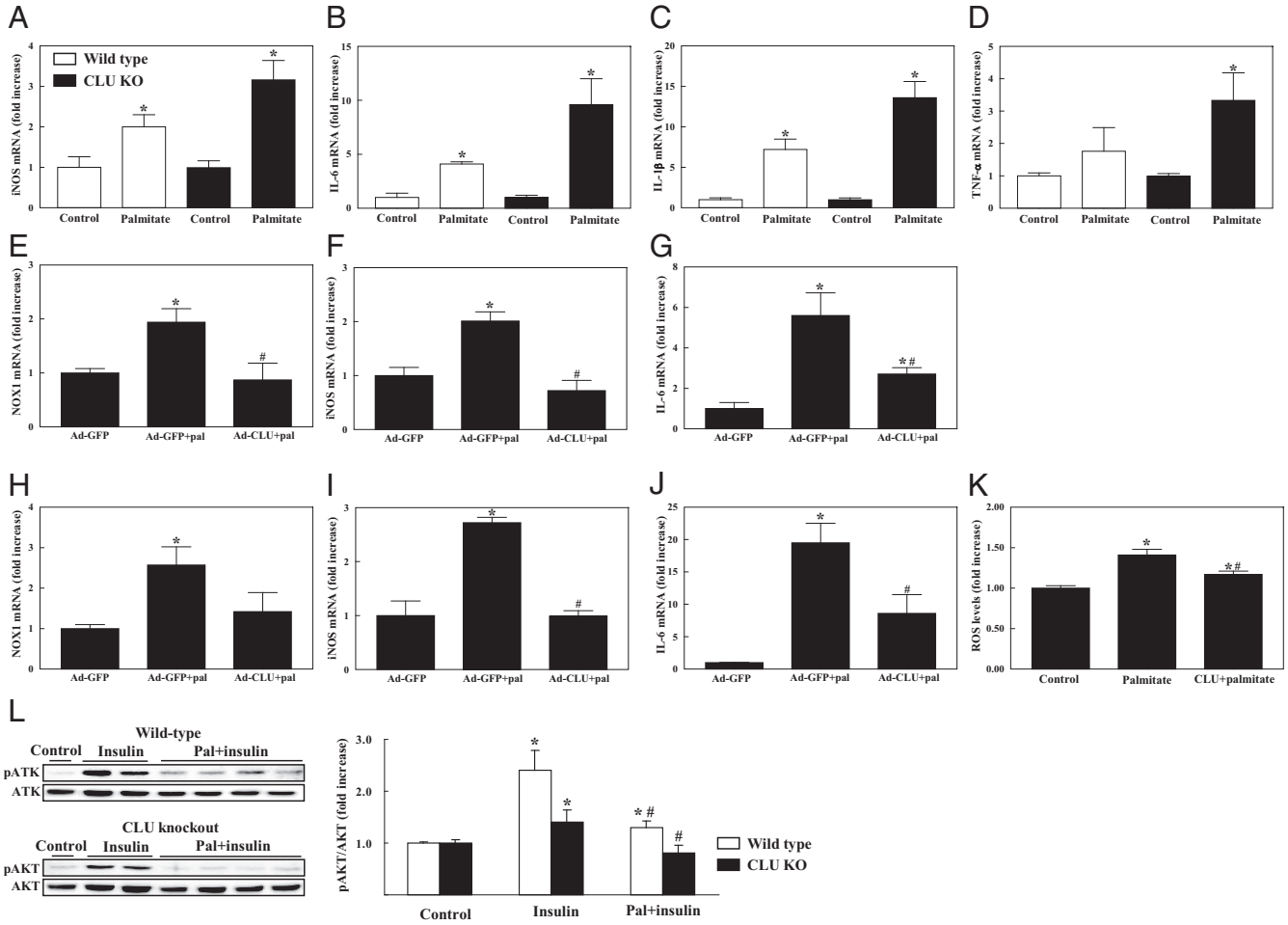

Figure 7. Effect of clusterin on palmitate-induced oxidative stress, inflammation, and AKT phosphorylation in the primary cultured hepatocytes and C2C12 myotubes. The hepatocytes from wild-type and clusterin knockout mice were treated with 500μM palmitate for 10 hours, and the gene expression of iNOS (A), IL-6 (B), IL-1β (C), and TNF-α (D) was measured. The hepatocytes from wild-type mice and differentiated C2C12 myotubes were treated with 1 plaque-forming unit per cell (pfu/cell) of Ad-GFP or clusterin (Ad-CLU) for 24 hours, and then treated with 500μM palmitate (Pal) for 10 hours. The gene expression of NOX1 (E and H), iNOS (F and I), and IL-6 (G and J) was measured. C2C12 cells were pretreated with 1 μg/mL clusterin for 1 hour before the treatment of 500μM palmitate for 6 hours. ROS generation was measured with flow cytometry (K). The hepatocytes from wild-type and clusterin knockout mice were treated with 500μM palmitate for 10 hours and then treated with 10nM insulin for 30 minutes. AKT phosphorylation at serine-473 was measured using Western blotting (L). The results are expressed as the mean ± SE of at least 3 separate experiments, each performed triplicate. *, $P < .05$ vs corresponding control or Ad-GFP, and #, $P < .05$ vs Ad-GFP+pal or insulin. CLU, clusterin; KO, knockout.

knockout mice also supports the association of clusterin deficiency with insulin resistance.

A hyperinsulinemic-euglycemic clamp study was conducted to define tissue-specific insulin resistance. However, we failed to observe a difference in insulin sensitivity between the 2 groups in the skeletal muscle and liver, which is incompatible with HOMA-IR and IPGTT data. Interestingly, the clamp insulin levels were significantly higher in high fat-fed clusterin knockout mice compared with the wild-type mice. When the clamp insulin levels are different among the comparison groups in the hyperinsulinemic-euglycemic clamp, the values can be adjusted with the clamp insulin levels (38, 39). For this adjustment, the clamp insulin level is assumed to be linearly related to insulin sensitivity (39). According to Ayala et al (40), insulin sensitivity is linearly related to the clamp insulin level within a range between 83pM and 1270pM. Because the clamp insulin levels in the present study were between 254 and 1170 pM, values that are within the range of the linear relationship between insulin sensitivity and insulin levels, we adjusted the values with the clamp insulin levels. The adjusted glucose infusion rate, glucose uptake, and suppression of HGP with the clamp insulin levels were significantly lower in the clusterin knockout mice, which are compatible with IPGTT and HOMA-IR data. These results suggest that a clusterin deficiency aggravates high-fat diet-induced insulin resistance. FBP and G6P are the key enzymes of HGP (41, 42), and the attenuated suppression of mRNA levels of these enzymes by insulin treatment in the high fat-fed clusterin knockout mice compared with

the high fat-fed wild-type mice also suggests an aggravated insulin resistance in the clusterin-deficient mice.

Increased insulin levels in clusterin knockout mice may be caused by increased insulin secretion. The increased C-peptide levels and islet size in the high fat-fed clusterin knockout mice support this notion. Moreover, most of the islet cells in the high fat-fed clusterin knockout mice were stained with insulin, suggesting that the increased insulin secretion may be caused by the increased β-cell numbers and/or functions. It seems that insulin secretion is increased to compensate for the peripheral insulin resistance in the high fat-fed clusterin knockout mice, and this speculation is supported by the fact that the insulin secretion in the chow diet group was not altered in this study. Because clusterin is also functionally implicated in the differentiation and regeneration of the β-cells (43, 44), the relationship between clusterin and insulin secretion needs to be clarified in a future study.

It has been proposed that clusterin is also involved in lipid metabolism, including lipid transportation and lipid synthesis (15, 45). Because lipid accumulation in peripheral tissues, such as in the skeletal muscle and liver, is associated with insulin resistance (46–48), we hypothesized that higher lipid levels might be responsible for aggravated insulin resistance in the clusterin knockout mice. However, although the high-fat diet increased triglyceride and total cholesterol levels in both the wild-type and clusterin knockout mice, the plasma and tissue levels of these lipids in the skeletal muscle and liver did not differ between the clusterin knockout mice and the wild-type mice. These results suggest that a deficiency of clusterin does not affect the lipid levels in the skeletal muscle and liver, and thus, aggravated insulin resistance in the high fat-fed clusterin knockout mice is not contributed by altered lipid metabolism in these tissues.

In summary, a deficiency of clusterin aggravates high-fat diet-induced insulin resistance through increased oxidative stress and inflammation, suggesting that clusterin plays a protective role in high-fat diet-induced insulin resistance. Clusterin may be a new therapeutic target for type 2 diabetes.

Acknowledgments

Address all correspondence and requests for reprints to: So-Young Park, Department of Physiology, Yeungnam University College of Medicine, Daegu 705–717, South Korea. E-mail: sypark@med.yu.ac.kr.

This work was supported by Basic Science Research Program through the National Research Foundation of Korea (NRF) funded by the Ministry of Education, Science and Technology (2005-0049417) and by a grant of the Korea Health Technology R&D Project, Ministry of Health and Welfare (A111345), Republic of Korea.

Disclosure Summary: The authors have nothing to disclose.

References

1. **de Silva HV, Stuart WD, Park YB, et al.** Purification and characterization of apolipoprotein J. *J Biol Chem*. 1990;265:14292–14297.
2. **Aronis KN, Kim YB, Mantzoros CS.** Clusterin (apolipoprotein J): wither link with diabetes and cardiometabolic risk? *Metabolism*. 2011;60:747–748.
3. **Bettuzzi S.** Conclusions and perspectives. *Adv Cancer Res*. 2009; 105:133–150.
4. **Jenne DE, Lowin B, Peitsch MC, Böttcher A, Schmitz G, Tschopp J.** Clusterin (complement lysis inhibitor) forms a high density lipoprotein complex with apolipoprotein A-I in human plasma. *J Biol Chem*. 1991;266:11030–11036.
5. **Trougakos IP, Gonos ES.** Clusterin/apolipoprotein J in human aging and cancer. *Int J Biochem Cell Biol*. 2002;34:1430–1448.
6. **Trougakos IP, Poulakou M, Stathatos M, Chalikia A, Melidonis A, Gonos ES.** Serum levels of the senescence biomarker clusterin/apolipoprotein J increase significantly in diabetes type II and during development of coronary heart disease or at myocardial infarction. *Exp Gerontol*. 2002;37:1175–1187.
7. **Rizzi F, Bettuzzi S.** Clusterin (CLU) and prostate cancer. *Adv Cancer Res*. 2009;105:1–19.
8. **Watari H, Ohta Y, Hassan MK, Xiong Y, Tanaka S, Sakuragi N.** Clusterin expression predicts survival of invasive cervical cancer patients treated with radical hysterectomy and systematic lymphadenectomy. *Gynecol Oncol*. 2008;108:527–532.
9. **Kujiraoka T, Hattori H, Miwa Y, et al.** Serum apolipoprotein j in health, coronary heart disease and type 2 diabetes mellitus. *J Atheroscler Thromb*. 2006;13:314–322.
10. **Hoofnagle AN, Wu M, Gosmanova AK, et al.** Low clusterin levels in high-density lipoprotein associate with insulin resistance, obesity, and dyslipoproteinemia. *Arterioscler Thromb Vasc Biol*. 2010;30: 2528–2534.
11. **Daimon M, Oizumi T, Karasawa S, et al.** Association of the clusterin gene polymorphisms with type 2 diabetes mellitus. *Metabolism*. 2011;60:815–822.
12. **Jung GS, Kim MK, Jung YA, et al.** Clusterin attenuates the development of renal fibrosis. *J Am Soc Nephrol*. 2012;23:73–85.
13. **McLaughlin L, Zhu G, Mistry M, et al.** Apolipoprotein J/clusterin limits the severity of murine autoimmune myocarditis. *J Clin Invest*. 2000;106:1105–1113.
14. **Sung HK, Sung HK, Kim YW, et al.** COMP-angiopoietin-1 enhances skeletal muscle blood flow and insulin sensitivity in mice. *Am J Physiol Endocrinol Metab*. 2009;297:E402–E409.
15. **Seo HY, Kim MK, Jung YA, et al.** Clusterin decreases hepatic SREBP-1c expression and lipid accumulation. *Endocrinology*. 2013;154:1722–1730.
16. **Song SE, Kim YW, Kim JY, Lee DH, Kim JR, Park SY.** IGFBP5 mediates high glucose-induced cardiac fibroblast activation. *J Mol Endocrinol*. 2013;50:291–303.
17. **Bae SK, Cha HN, Ju TJ, et al.** Deficiency of inducible nitric oxide synthase attenuates immobilization-induced skeletal muscle atrophy in mice. *J Appl Physiol*. 2012;113:114–123.
18. **Folch J, Lees M, Sloane Stanley GH.** A simple method for the isolation and purification of total lipides from animal tissues. *J Biol Chem*. 1957;226:497–509.
19. **Frippiat C, Chen QM, Zdanov S, Magalhaes JP, Remacle J, Toussaint O.** Subcytotoxic H2O2 stress triggers a release of transforming

growth factor-β 1, which induces biomarkers of cellular senescence of human diploid fibroblasts. *J Biol Chem*. 2001;276:2531–2537.
20. **Calvo EL, Mallo GV, Fiedler F, et al.** Clusterin overexpression in rat pancreas during the acute phase of pancreatitis and pancreatic development. *Eur J Biochem*. 1998;254:282–289.
21. **Viard I, Wehrli P, Jornot L, et al.** Clusterin gene expression mediates resistance to apoptotic cell death induced by heat shock and oxidative stress. *J Invest Dermatol*. 1999;112:290–296.
22. **Hardardóttir I, Kunitake ST, Moser AH, et al.** Endotoxin and cytokines increase hepatic messenger RNA levels and serum concentrations of apolipoprotein J (clusterin) in Syrian hamsters. *J Clin Invest*. 1994;94:1304–1309.
23. **Boden MJ, Brandon AE, Tid-Ang JD, et al.** Overexpression of manganese superoxide dismutase ameliorates high-fat diet-induced insulin resistance in rat skeletal muscle. *Am J Physiol Endocrinol Metab*. 2012;303:E798–E805.
24. **Riant E, Waget A, Cogo H, Arnal JF, Burcelin R, Gourdy P.** Estrogens protect against high-fat diet-induced insulin resistance and glucose intolerance in mice. *Endocrinology*. 2009;150:2109–2117.
25. **Jordan-Starck TC, Lund SD, Witte DP, et al.** Mouse apolipoprotein J: characterization of a gene implicated in atherosclerosis. *J Lipid Res*. 1994;35:194–210.
26. **Laping NJ, Olson BA, Day JR, et al.** The age-related increase in renal clusterin mRNA is accelerated in obese Zucker rats. *J Am Soc Nephrol*. 1998;9:38–45.
27. **Monte SV, Caruana JA, Ghanim H, et al.** Reduction in endotoxemia, oxidative and inflammatory stress, and insulin resistance after Roux-en-Y gastric bypass surgery in patients with morbid obesity and type 2 diabetes mellitus. *Surgery*. 2012;151:587–593.
28. **Ghanim H, Monte SV, Sia CL, et al.** Reduction in inflammation and the expression of amyloid precursor protein and other proteins related to Alzheimer's disease following gastric bypass surgery. *J Clin Endocrinol Metab*. 2012;97:E1197–E1201.
29. **Savkovi V, Gantzer H, Reiser U, et al.** Clusterin is protective in pancreatitis through anti-apoptotic and anti-inflammatory properties. *Biochem Biophys Res Commun*. 2007;356:431–437.
30. **Dumont P, Chainiaux F, Eliaers F, et al.** Overexpression of apolipoprotein J in human fibroblasts protects against cytotoxicity and premature senescence induced by ethanol and tert-butylhydroperoxide. *Cell Stress Chaperones*. 2002;7:23–35.
31. **Miyake H, Hara I, Gleave ME, Eto H.** Protection of androgen-dependent human prostate cancer cells from oxidative stress-induced DNA damage by overexpression of clusterin and its modulation by androgen. *Prostate*. 2004;61:318–323.
32. **Lee YN, Shim YJ, Kang BH, Park JJ, Min BH.** Over-expression of human clusterin increases stress resistance and extends lifespan in *Drosophila* melanogaster. *Biochem Biophys Res Commun*. 2012; 420:851–856.
33. **Van Linthout S, Spillmann F, Riad A, et al.** Human apolipoprotein A-I gene transfer reduces the development of experimental diabetic cardiomyopathy. *Circulation*. 2008;117:1563–1573.
34. **Stuart WD, Krol B, Jenkins SH, Harmony JA.** Structure and stability of apolipoprotein J-containing high-density lipoproteins. *Biochemistry*. 1992;31:8552–8559.
35. **Evans JL, Goldfine ID, Maddux BA, Grodsky GM.** Oxidative stress and stress-activated signaling pathways: a unifying hypothesis of type 2 diabetes. *Endocr Rev*. 2002;23:599–622.
36. **Yuzefovych L, Wilson G, Rachek L.** Different effects of oleate vs. palmitate on mitochondrial function, apoptosis, and insulin signaling in L6 skeletal muscle cells: role of oxidative stress. *Am J Physiol Endocrinol Metab*. 2010;299:E1096–E1105.
37. **Styskal J, Nwagwu FA, Watkins YN, et al.** Methionine sulfoxide reductase A affects insulin resistance by protecting insulin receptor function. *Free Radic Biol Med*. 2013;56:123–132.
38. **Boden G, Sargrad K, Homko C, Mozzoli M, Stein TP.** Effect of a low-carbohydrate diet on appetite, blood glucose levels, and insulin resistance in obese patients with type 2 diabetes. *Ann Intern Med*. 2005;142:403–411.
39. **Ayala JE, Bracy DP, Malabanan C, et al.** Hyperinsulinemic-euglycemic clamps in conscious, unrestrained mice. *J Vis Exp*. 2011; 16.pii:3188.
40. **Ayala JE, Bracy DP, McGuinness OP, Wasserman DH.** Considerations in the design of hyperinsulinemic-euglycemic clamps in the conscious mouse. *Diabetes*. 2006;55:390–397.
41. **Andrikopoulos S, Proietto J.** The biochemical basis of increased hepatic glucose production in a mouse model of type 2 (non-insulin-dependent) diabetes mellitus. *Diabetologia*. 1995;38:1389–1396.
42. **Sun Y, Liu S, Ferguson S, et al.** Phosphoenolpyruvate carboxykinase overexpression selectively attenuates insulin signaling and hepatic insulin sensitivity in transgenic mice. *J Biol Chem*. 2002;277: 23301–23307.
43. **Kim BM, Kim SY, Lee S, et al.** Clusterin induces differentiation of pancreatic duct cells into insulin-secreting cells. *Diabetologia*. 2006; 49:311–320.
44. **Kim BM, Han YM, Shin YJ, Min BH, Park IS.** Clusterin expression during regeneration of pancreatic islet cells in streptozotocin-induced diabetic rats. *Diabetologia*. 2001;44:2192–2202.
45. **Gelissen IC, Hochgrebe T, Wilson MR, et al.** Apolipoprotein J (clusterin) induces cholesterol export from macrophage-foam cells: a potential anti-atherogenic function? *Biochem J*. 1998;331(pt 1): 231–237.
46. **Kim JK, Fillmore JJ, Chen Y, et al.** Tissue-specific overexpression of lipoprotein lipase causes tissue-specific insulin resistance. *Proc Natl Acad Sci USA*. 2001;98:7522–7527.
47. **Turner N, Kowalski GM, Leslie SJ, et al.** Distinct patterns of tissue-specific lipid accumulation during the induction of insulin resistance in mice by high-fat feeding. *Diabetologia*. 2013;56:1638–1648.
48. **Hwang JH, Stein DT, Barzilai N, et al.** Increased intrahepatic triglyceride is associated with peripheral insulin resistance: in vivo MR imaging and spectroscopy studies. *Am J Physiol Endocrinol Metab*. 2007;293:E1663–E1669.